THE ASTROPHYSICAL JOURNAL, 436:L41–L45, 1994 November 20

DETECTIONS OF HARD X-RAY EMISSIONS FROM BRIGHT EARLY-TYPE GALAXIES WITH *ASCA*

K. MATSUSHITA,[1] K. MAKISHIMA,[1] H. AWAKI,[2] C. R. CANIZARES,[3] A. C. FABIAN,[4] Y. FUKAZAWA,[1]
M. LOEWENSTEIN,[5] H. MATSUMOTO,[2] T. MIHARA,[6] R. F. MUSHOTZKY,[5] T. OHASHI,[7] G. R. RICKER,[3]
P. J. SERLEMITSOS,[5] T. TSURU,[2] Y. TSUSAKA,[8] AND T. YAMAZAKI[8]
Received 1994 June 2; accepted 1994 August 29

ABSTRACT

Five bright elliptical galaxies in the Virgo Cluster, NGC 4365, NGC 4374 (M84), NGC 4406 (M86), NGC 4472 (M49), and NGC 4636, were observed with *ASCA*. In addition to the extended thermal X-ray emission of temperature $kT \sim 1$ keV, harder X-rays with color temperature $kT \geq 2$ keV were detected from all of them. The 2–10 keV luminosities of this hard component for the five galaxies, integrated within 5′, are distributed within a relatively narrow range of $(1–4) \times 10^{40}$ ergs s^{-1}. The hard X-ray component is primarily attributed to the integrated emission from discrete X-ray sources. In NGC 4406 and NGC 4374 the data indicate that the hard component is contributed additionally by foreground/background emission from the hot intracluster medium (ICM) of the Virgo Cluster. The hard component of NGC 4472 seems also contributed by the Virgo ICM emission, but in this case there is evidence that the ICM brightness is locally enhanced within $\sim 10'$ of NGC 4472.

Subject headings: galaxies: clusters of — galaxies: elliptical and lenticular, cD — X-rays: galaxies — X-rays: ISM

1. INTRODUCTION

Elliptical galaxies are often strong sources of extended thermal X-ray emission, as revealed first by the *Einstein Observatory* (Forman et al. 1979; Forman, Jones, & Tucker 1985, hereafter FJT85; Trinchieri, Fabbiano, & Canizares 1986, hereafter TFC86; Canizares, Fabbiano, & Trinchieri 1987, hereafter CFT87; Fabbiano 1989) and then by *Ginga* (Awaki et al. 1991), *ROSAT* (Forman et al. 1993; Trinchieri et al. 1994; Pellegrini & Fabbiano 1994) and BBXRT (Serlemitsos et al. 1993, hereafter SEA93). The bulk of these X-rays are emitted from a thin hot interstellar medium (ISM) of temperature ~ 1 keV, and the total mass necessary to confine them provides solid evidence for dark matter in these systems.

Many elliptical galaxies are immersed in a cluster environment, where X-ray–emitting large-scale intracluster medium (ICM) is distributed. Because of the deeper gravitational potential of the entire cluster, the ICM is usually hotter than the hot ISM of individual elliptical galaxies. The relation between the ICM and the ISM bears important clues as to formation and chemical evolution of the cluster and its member galaxies, and also provides valuable insight into variations of dark-to-luminous matter ratios from the local vicinity of member galaxies to the entire cluster. However, the relation between these two types of hot gaseous components has not yet been very well understood.

Through *ASCA* observations of five elliptical galaxies in the Virgo Cluster, we have detected not only the soft thermal X-rays from the hot ISM, but also an additional X-ray component whose temperature is as high as those of the Virgo ICM emission. We discuss possible origins of this hard component.

2. OBSERVATIONS

We here investigate X-ray emission from five optically bright elliptical galaxies in the Virgo Cluster; the sample consists of three X-ray–bright systems NGC 4406, NGC 4472, and NGC 4636; one X-ray faint object NGC 4365; and an intermediate object NGC 4374. As summarized in Table 1, all these objects were observed with *ASCA* (Tanaka et al. 1994) during the performance verification phase, and detailed plasma diagnostics using the SIS data from these same observations have already been reported by Awaki et al. (1994, hereafter AEA94) for the X-ray bright three objects. In this *Letter* we mainly analyze the GIS data (all acquired in normal PH mode) which have better statistics than the SIS data above 3–4 keV, in an attempt to quantify wide-band X-ray properties of these five galaxies.

Figure 1 (Plate L1) shows two-color GIS X-ray images of the three fields containing four target galaxies. They include non–X-ray background (NXB), cosmic X-ray background (CXB), and the Virgo ICM emission. The images confirm the extended X-ray emission from these galaxies as observed previously, and the observed X-ray intensities in Table 1 generally agree with previous measurements (e.g., FJT85; TFC86; CFT87).

3. SPECTRAL ANALYSIS AND RESULTS

We accumulated on-source spectra within a 5′ radius centered on each galaxy for the two GIS detectors (called GIS2

[1] Department of Physics, University of Tokyo, 7-3-1 Hongo, Bunkyo-ku, Tokyo, Japan 113.
[2] Department of Physics, Kyoto University, Sakyo-ku, Kyoto, Japan 606-01.
[3] Center for Space Research, Massachusetts Institute of Technology, Cambridge, MA 02193.
[4] Institute of Astronomy, University of Cambridge, Cambridge, CB3 0HA, UK.
[5] Laboratory of High Energy Physics, NASA/GSFC, Greenbelt, MD 20771.
[6] Cosmic Ray Laboratory, Institute of Physical and Chemical Research, Wako, Saitama, Japan 350-01.
[7] Department of Physics, Tokyo Metropolitan University, Hachioji, Tokyo, Japan 192-03.
[8] Department of Physics, Nagoya University, Furo-cho, Chikusa-ku, Nagoya, Japan 464-01.

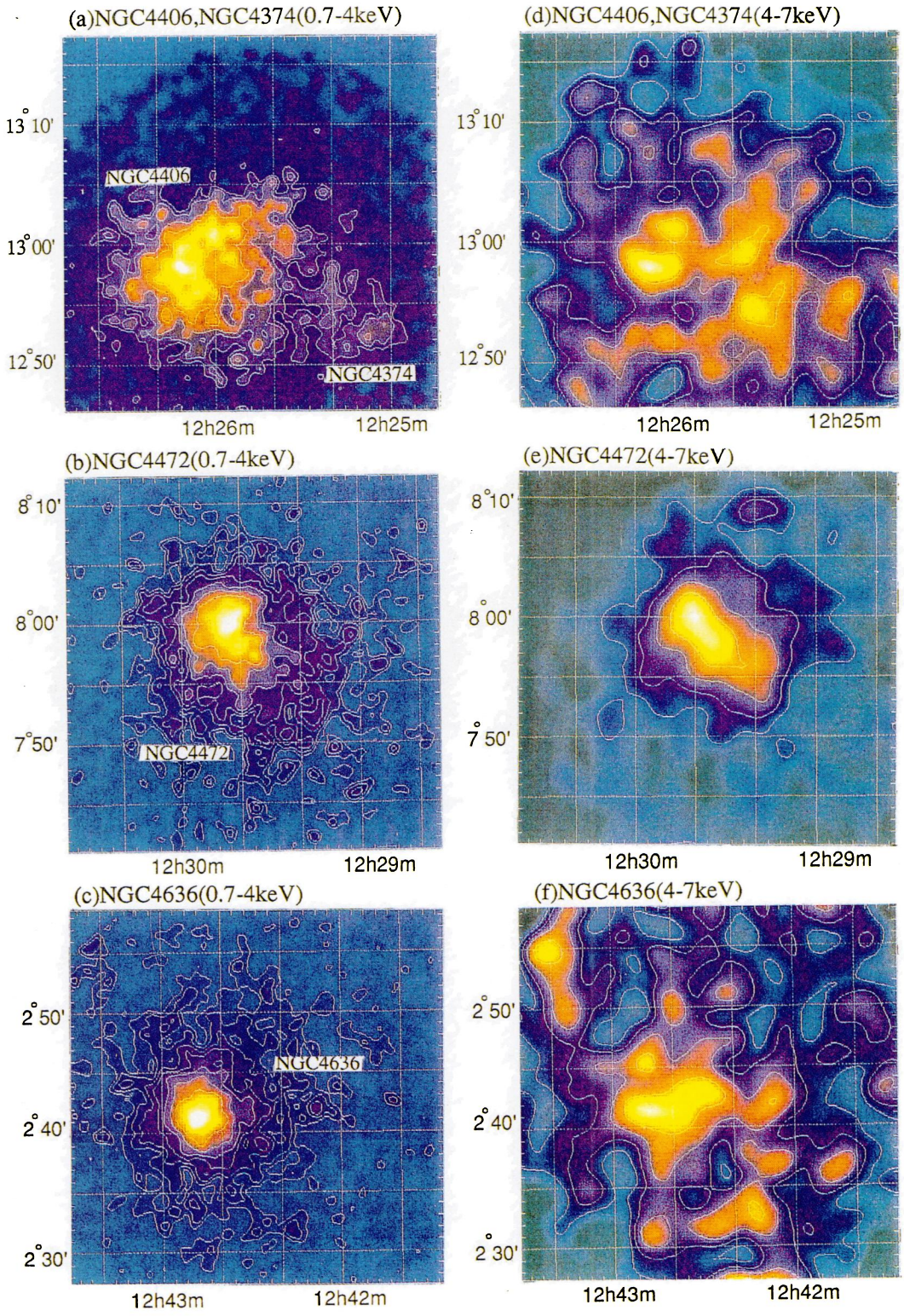

FIG. 1.—Pseudocolor GIS (GIS2 plus GIS3) images of the three fields in the Virgo Cluster, containing four of the five target galaxies. Panels (*a*), (*b*), and (*c*) are for NGC 4406 + NGC 4374, NGC 4472, and NGC 4636, respectively, in the 0.7–4 keV energy band, after smoothing with a Gaussian of $\sigma = 0.'38$. Panels (*d*)–(*f*) are the same as panels (*a*)–(*c*) respectively, but for the 4–7 keV band, after smoothing with a Gaussian of $\sigma = 1.'25$. All the images include background and the Virgo Cluster emission. They are not corrected for the telescope vignetting or partial shadows due to the GIS window support ribs. For panel (*a*), 20%–100% of the peak brightness is logarithmically divided into eight levels, while for panels (*b*) and (*c*), 5%–100% of the peak brightness is similarly divided into six levels. For panels (*d*)–(*f*), 30%–100% of the peak brightness is logarithmically divided into four levels.

MATSUSHITA et al. (see 436, L41)

TABLE 1

LOG OF *ASCA* OBSERVATIONS OF ELLIPTICAL GALAXIES AND RESULTS OF THE SINGLE-TEMPERATURE RAYMOND-SMITH FIT TO THE GIS (GIS2 + GIS3) SPECTRA[a,b]

Target NGC	Date of Observation (1993)	Exposure (ks)	SIS/GIS (counts s^{-1})[c]	kT (keV)	Abundance (solar)	χ^2/ν
4365.....	Jun 28	30	0.015/0.015	3.1 ± 0.9	0.7 (0.0–2.0)	37/28
4374.....	Jul 4	19	0.15/0.067	1.6 ± 0.2	0.2 (0.1–0.5)	113/51
4406.....	Jul 3	13	0.37/0.16	0.82 ± 0.03	0.22 (0.16–0.29)	127/72
4472.....	July 4	13	0.22/0.16	$0.94^{+0.04}_{-0.11}$	0.36 (0.18–0.50)	180/73
4636.....	Jun 22	25	0.23/0.10	0.74 ± 0.03	0.27 (0.20–0.38)	199/88

[a] Errors represent single-parameter 90% confidence limits, although not very meaningful as the fits are not acceptable. See text for the fitting condition.

[b] Data have been integrated within a radius of 5′.

[c] Signal counting rates within 5′ radius in 0.5–5 keV for the SIS and 0.7–7 keV for the GIS, excluding the cosmic X-ray background and the particle background, but including the Virgo Cluster emission. Difference between the GIS and the SIS rates is mainly due to differences in their spectral passbands.

and GIS3; Kohmura et al. 1993; Ohashi et al. 1994) separately. To remove the NXB and CXB, for each detector we subtracted a background spectrum which was accumulated over the same region using the Draco field data obtained on 1993 June 4–5. A reliable background subtraction was achieved by discarding data acquired under magnetic cutoff rigidities <10 GeV. The GIS spectra thus obtained are shown in Figures 2 and 3; note that the Virgo ICM emission is not subtracted. At 0.8–1, 1.3–1.4, and $\sim$1.8 keV of the spectra, we see iron L-line complex, Mg Kα line, and Si Kα line, respectively, which characterize emission from $kT \sim 1$ keV plasmas.

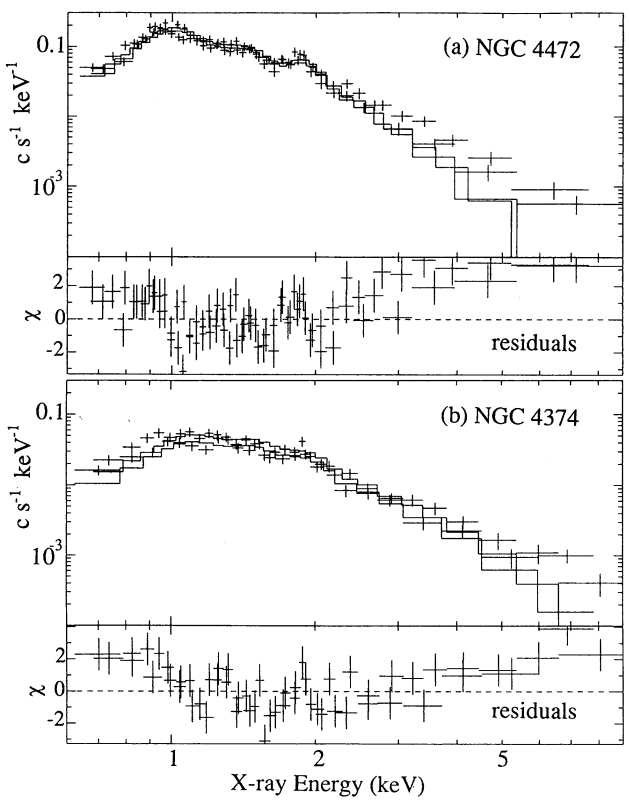

FIG. 2.—The GIS spectra of (*a*) NGC 4472 and (*b*) NGC 4374, fitted with a single-temperature Raymond-Smith emission model. The same model convolved through responses of the GIS2 and the GIS3 detectors are fitted to respective spectra. The fit parameters are shown in Table 1.

For each galaxy, we first fitted the spectra with a single-temperature ionization equilibrium plasma emission model due to Raymond & Smith (1977), modified by photoelectric absorption, using the XSPEC data analysis package version 8.41. The metal abundances are left free while keeping the solar ratios, taking the solar iron abundance (by the number ratio) to be 4.68×10^{-5}. The absorption N_H was first fixed at the values obtained by AEA94 for the brighter three objects, and at the Galactic value for the other two (see Table 2 for detail). Because the instrumental response slightly differs between GIS2 and GIS3, we fitted their spectra separately using a common model. The results of this analysis are summarized in Table 1. The temperature turned out to be 0.7–1.6 keV except for NGC 4365, in gross agreement with previous results (FJT85; TFC86; CFT87; SEA93; Forman et al. 1993; Kim, Fabbiano, & Trinchieri 1992a; Trinchieri et al. 1994).

However, none of these fits are acceptable, and letting N_H float did not improve the fit at all. The fits suffer from significant positive residuals above $\sim$3 keV as exemplified in Figure 2. The fits are much improved when the fit energy range is restricted either to <4 keV or to >2.5 keV, but in the latter case the derived temperature tends to be rather high (2.5–3.5 keV). These suggest the presence of an emission component, to be called the "hard component," which is significantly harder than the well-established $kT \sim 1$ keV "soft component." At a representative energy of 5 keV, the spectral excess attributable to this hard component amounts to $\sim 10^{-3}$ counts s^{-1} keV^{-1} in all five galaxies. This is comparable to the total (NXB plus CXB) GIS background for a 5′ radius region, which, however, can be reproduced within a typical uncertainty of $\leq 5\%$. Therefore the hard component must be real rather than due to incorrect background subtraction. This conclusion is supported by the fact that at least NGC 4406, NGC 4472 and NGC 4636 are clearly visible in Figure 1 above 4 keV, where the hard component dominates the emission. The apparently high temperature of NGC 4365 (and of NGC 4374, too) suggests that the emission from these X-ray fainter systems in the *ASCA* band (0.5–10 keV) is dominated by the hard component.

We next fitted the spectra with a sum of two Raymond-Smith models with different temperatures and normalizations but common abundances, representing the soft and the hard components. Since the GIS data alone cannot determine absorption very well, for the soft component of the X-ray brightest three galaxies, we fixed N_H to the values derived by AEA94 using the SIS data, and for the fainter two to the line-

of-sight Galactic value of 3×10^{20} cm^{-2}. For the hard component we assume the Galactic line-of-sight absorption. The two-temperature fit has mostly been successful (Table 2, Fig. 3), which confirms that the hard component is statistically significant. For all the objects, however, only lower limits on the hard-component temperature kT_h have been obtained (Table 2). As a result, the hard component flux is subject to uncertainties typically by factors of 3, 1.5, and 2 at energies of 2, 4, and 6 keV, respectively. Within these uncertainties, the hard component fluxes thus obtained for the X-ray brightest three galaxies are consistent with those obtained by AEA94 using the SIS data, and also with the lack of excess hard emission in the BBXRT spectrum of NGC 4472 (SEA93) having a much shorter integration time. The GIS data can constrain the hard component much more tightly than the SIS data.

The soft component temperatures have been determined to be $kT_s = 0.7$–1.0 keV for all the five galaxies. Therefore a small amount of hot ISM exists even in the X-ray–faint NGC 4365, although the GIS is insensitive to the very soft ($kT \sim 0.2$ keV) component detected with *ROSAT* (Pellegrini & Fabbiano 1994). The values of kT_s for the X-ray brightest objects are only slightly lower than those found in the single-temperature fits. The soft component metallicity has been constrained with a reasonable accuracy, reconfirming that the hot ISM in elliptical galaxies are relatively devoid of heavy elements (Awaki et al. 1991; Forman et al. 1993; SEA93; AEA94). More quantitatively, our soft-component parameters for NGC 4406, NGC 4472, and NGC 4636 are consistent with those derived by AEA94, and those for NGC 4374 with the results of Loewenstein et al. (1994) within respective errors. However, the metallicity estimates are considerably model dependent, because the uncertainty in the hard component flux propagates into that in the continuum flux attributable to the soft component, hence into that of the metallicity. For example, replacing the hotter Raymond-Smith model with a thermal bremsstrahlung model considerably raises the upper bound on the metallicity for smaller values of kT_h. Further analysis involving the joint SIS/GIS fitting will be reported in a later publication.

4. DISCUSSION

We have detected hard ($kT_h \geq 2$ keV) X-ray emission from the five Virgo ellipticals, in addition to the soft ($kT_s \sim 1$ keV) plasma emission due to the hot ISM. While the soft component

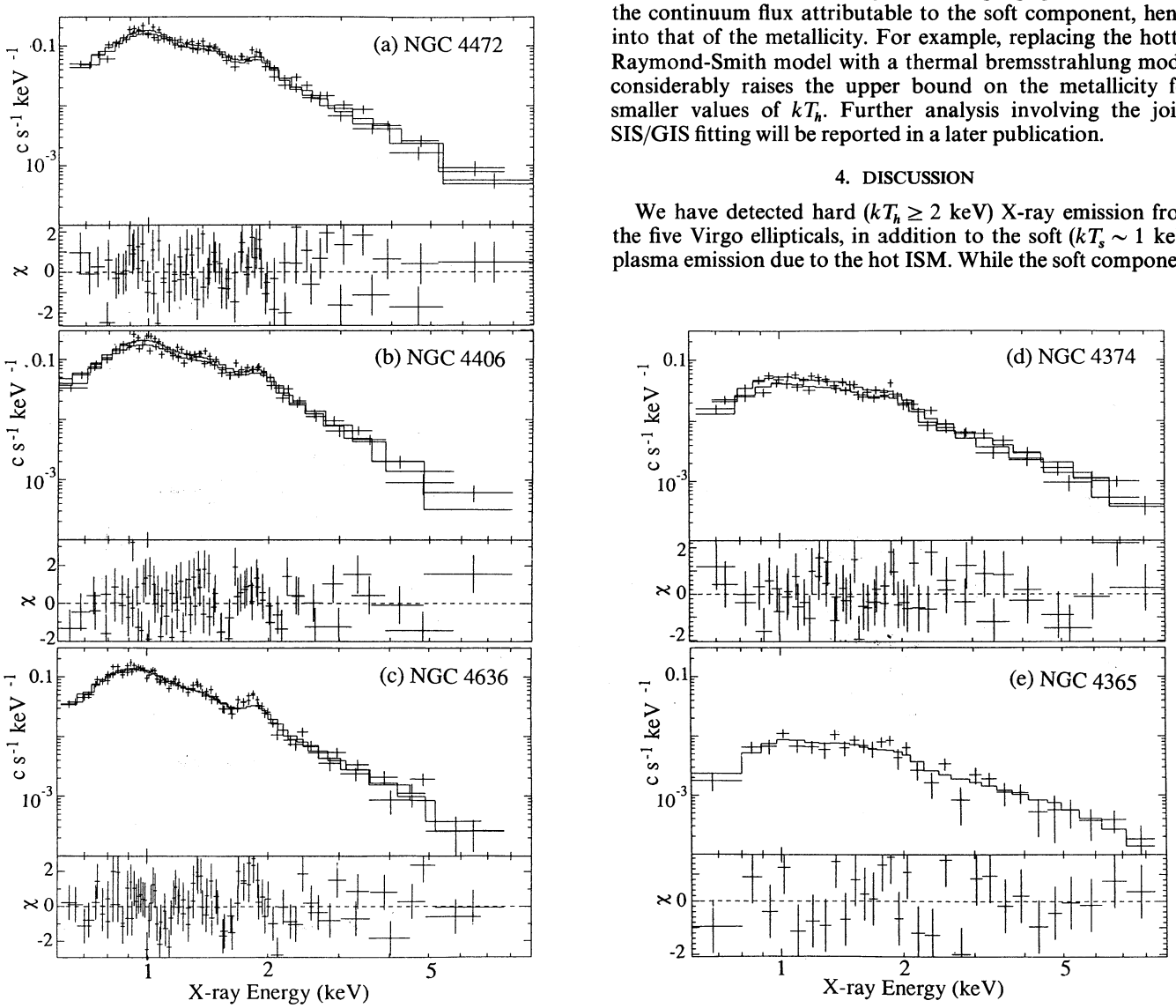

FIG. 3.—The GIS spectra of (*a*) NGC 4472, (*b*) NGC 4406, (*c*) NGC 4636, (*d*) NGC 4374, and (*e*) NGC 4365, fitted with a spectrum consisting of two Raymond-Smith models of common abundances. Panels (*a*) and (*d*) are the same as panels (*a*) and (*b*) of Fig. 2, except for the difference in the fitted model. The hard-component temperature kT_h is fixed for display at a representative value of 4 keV. The best-fit parameters are given in Table 2. For NGC 4365, the G1S2 and the GIS3 spectra are added together before the fitting, since the difference in the GIS2 and GIS3 responses is well within statistical uncertainties of the data in this particular case.

TABLE 2

RESULTS OF THE SPECTRAL FITS USING TWO RAYMOND-SMITH MODELS[a]

TARGET NGC	SOFT X-RAY COMPONENT				HARD X-RAY COMPONENT			FIT
	kT_s (keV)	N_H[b]	log L_s[c]	Abundance[d]	kT_h (keV)	log L_h[c]	log L_d[c]	χ^2/ν
4365.....	$1.0^{+0.4}_{-0.3}$	(0.3)	39.94	0.38 (0.0–2.0)	7.2 (>2.7)	40.06	39.95	28/26
4374.....	0.85 ± 0.16	(0.3)	40.74	0.06 (0.02–0.13)	9.2 (>4.0)	40.54	40.12	46/49
4406.....	$0.78^{+0.05}_{-0.03}$	1.0	41.38	0.40 (0.18–0.42)	3.7 (>1.9)	40.38	40.20	92/70
4472.....	0.83 ± 0.04	1.2	41.32	0.42 (0.26–0.77)	4.4 (>2.7)	40.59	40.47	89/71
4636.....	0.70 ± 0.03	0.7	41.24	0.41 (0.28–0.63)	4.5 (>2.7)	40.23	40.01	136/86

[a] Errors represent single-parameter 90% confidence limits.

[b] The absorbing column density in units of 10^{21} cm^{-2}, taken from AEA94 for NGC 4406, NGC 4472, and NGC 4636, and fixed to the Galactic value of 0.3 for the remaining two.

[c] The 0.5–5 keV luminosity of the soft component L_s and the 2–10 keV luminosity of the hard component L_h, assuming a distance of 17 Mpc.

[d] Best-fit values and the 90% ranges of the abundance, assumed to be of the solar ratios and to be the same for the two components.

[e] The 2–10 keV luminosity expected for the discrete sources, at a distance of 17 Mpc (from CFT87).

luminosities scatter by a factor of $\sim$28 among the five targets, their hard component luminosities L_h are similar within a factor of $\sim$4 (see Table 2). A similar hard component has also been found in preliminary *ASCA* spectra of two ellipticals outside the Virgo Cluster, NGC 720 and IC 1459 (Matshusita & Makashima 1994), as well as in the BBXRT spectra of NGC 1399 (SEA93). Therefore the hard X-ray component can be considered to be a relatively common property of the elliptical galaxies.

Statistical studies using the *Einstein* data (CFT87; Kim, Fabbiano, & Trinchieri 1982b) have revealed the presence of a hard X-ray component underlying the X-ray emission from elliptical galaxies, and attributed it to integrated emission from discrete X-ray sources. Our hard component can primarily be identified with this component, because the measured values of L_h are very close to the discrete-source contribution, L_d (Table 2), estimated by CFT87 based on X-ray luminosities of spiral galaxies. The temperature of $kT_h \geq 2$ keV is also consistent with that for the average discrete-source spectrum (Kim et al. 1992b; cf. $kT \sim 7$ keV for M31, Makishima et al. 1989). We thus conclude that the discrete sources give a major contribution to the hard component observed with *ASCA* from all the five galaxies. (In the case of NGC 4374, there might be additional contribution from the radio-emitting nucleus.) This also implies that the integrated X-ray luminosity from binary X-ray sources is similar between elliptical galaxies and the bulge region of spiral galaxies, when scaled to the optical *B*-band luminosity (CFT87).

In some cases, however, the discrete sources alone cannot account for all the hard X-ray flux detected with *ASCA*. For example, in NGC 4406 which is located near the central Virgo Cluster, the hard component profile is much more extended than the soft component profile, keeping an almost constant brightness up to $\sim$20′ (Matsushita & Makishima 1994). In this case there must be an additional extended source of hard X-ray emission, most likely the Virgo ICM since we have subtracted only the CXB and the NXB when producing the spectra. Our values of kT_h are consistent with the temperature of the Virgo emission, 2.5–3 keV (Koyama, Takano, & Tawara 1991; Böringer et al. 1994). We have further confirmed that the ICM surface brightness, derived either with the GIS at a location between M87 and NGC 4406 or with the *Ginga* scan data (Takano et al. 1989), and integrated within the 5′ radius, can explain $\sim$50%–150% of the hard component of NGC 4406. The same conclusion has been reached for NGC 4374 by Loewenstein et al. (1994) who independently analyzed the *ASCA* data. We therefore conclude that a considerable fraction of the hard component of NGC 4406 and NGC 4374 comes from the background/foreground Virgo ICM emission. This may explain a relatively large L_h/L_d ratio of NGC 4374. Quantitative separation of the discrete-source contribution and the ICM contribution must await more detailed analysis of the *ASCA* images.

The case of NGC 4472 is somewhat similar. Its hard-band image (Fig. 1*e*) is elongated and displaced from the optical galaxy as well as from the soft-band image. Since such a distribution cannot be explained by the discrete sources, we infer that the hard component of this galaxy is also contributed by the ICM emission. This is reasonable because NGC 4472 sits in a region where the ICM emission is locally enhanced when observed with a $\sim$1° beam of the *Ginga* LAC (Takano et al. 1989). However, the ICM brightness measured with *Ginga* around NGC 4472, when rescaled for the 5′ circle, can explain only $<$10% of the hard X-ray flux from NGC 4472 observed with *ASCA*. Therefore, the ICM brightness must be locally enhanced around NGC 4472 over an angular scale considerably smaller than the *Ginga* beam. This is consistent with our hard X-ray image of NGC 4472, which is clearly localized within $\sim$10′ of NGC 4472. Similar effects were found with *ROSAT* around NGC 4472 and NGC 4406 (Böhringer et al. 1994). Thus the hard component of NGC 4472 may be explained as a sum of the discrete-source emission and the locally enhanced ICM emission, although their relative dominance remains unspecified at present.

The local irregularity in the ICM brightness, as observed around NGC 4472, may be caused by several mechanisms. One is due to real enhancement in the ICM *pressure*, in response to local structures in the cluster-wide gravitational potential, such as subclustering structures and potential dimples around bright ellipticals. Another possibility is that the ICM gets slightly cooler around each galaxy than the average, producing a local enhancement in the ICM *density* (but not in pressure); the associated temperature gradient would be masked by the soft component. Alternatively we may be observing some transient phenomenon; a part of the ISM emitting the soft component may be stripped off the galaxy by the ram pressure, become heated, and dissipate into the ICM, because the ISM moving together with the galaxy through the

cluster must have a specific energy comparable to the cluster's virial temperature and hence to the ICM temperature (cf. Trinchieri et al. 1994).

In summary, we have detected hard X-ray emission from five elliptical galaxies in the Virgo Cluster, employing the wide-band sensitivity of *ASCA*. The hard component is contributed by the discrete binary X-ray sources, and in some cases also by the hot ($kT = 2$–3 keV) ICM in the Virgo Cluster. The latter may come not only through the form of foreground/background emission but also though local enhancement in the ICM emissivity.

REFERENCES

Awaki, H., et al. 1994, PASJ, 46, L65 (AEA94)
Awaki, H., Koyama, K., Kunieda, H., Takano, S., Tawara, Y., & Ohashi, T. 1991, ApJ, 366, 88
Böhringer, H., Briel, U. G., Schwarz, R. A., Voges, W., Hartner, G., & Trümper, J. 1994, Nature, 368, 828
Canizares, C. R., Fabbiano, G., & Trinchieri, G. 1987, ApJ, 312, 503 (CFT87)
Fabbiano, G. 1989, ARA&A, 27, 87
Forman, W., Jones, C., David, L., Franx, M., Makishima, K., & Ohashi, T. 1993, ApJ, 418, L55
Forman, W., Jones, C., & Tucker, W. 1985, ApJ, 293, 102 (FJT85)
Forman, W., Schwarz, J., Jones, C., Liller, W., & Fabian, A. 1979, ApJ, 234, L27
Kim, D.-W., Fabbiano, G., & Trinchieri, G. 1992a, ApJS, 80, 645
———. 1992b, ApJ, 393, 134
Kohmura, Y., et al. 1993, Proc. SPIE, 2006, 79
Koyama, K., Takano, S., & Tawara, Y. 1991, Nature, 350, 135
Loewenstein, M., et al. 1994, ApJ, 436, L75
Makishima, K., et al. 1989, PASJ, 41, 697
Matsushita, K., & Makishima, K. 1994, in Proc. New Horizons of X-ray Astronomy, ed. F. Makino & T. Ohashi, in press
Ohashi, T., et al. 1994, PASJ, submitted
Pellegrini, S., & Fabbiano, G. 1994, ApJ, 429, 105
Raymond, J. C., & Smith, B. W. 1977, ApJS, 35, 419
Serlemitsos, P., Lowenstein, M., Mushotzky, R. F., Marshall, F. E., & Petre, R. 1993, ApJ, 413, 518 (SEA93)
Takano, S., et al. 1989, Nature, 340, 289
Tanaka, Y., et al. 1994, PASJ, 46, L37
Trinchieri, G., Fabbiano, G., & Canizares, C. R. 1986, ApJ, 310, 637 (TFC86)
Trinchieri, G., Kim, W.-D., Fabbiano, G., & Canizares, C. R. 1994, ApJ, 428, 555